

## Concerning the Localization of End Groups in Dendrimers

Anton W. Bosman,<sup>†</sup> Monique J. Bruining,<sup>†</sup> Huub Kooijman,<sup>‡</sup>  
Anthony L. Spek,<sup>‡</sup> René A. J. Janssen,<sup>†</sup> and E. W. Meijer<sup>\*,†</sup>

Laboratory of Macromolecular and Organic Chemistry  
Eindhoven University of Technology, PO Box 513  
5600 MB Eindhoven, The Netherlands  
Bijvoet Center for Biomolecular Research, Crystal  
Structural Chemistry, Utrecht University  
Padualaan 8, 3584 CH, Utrecht, The Netherlands

Received May 11, 1998

Theoretical investigations predicting the molecular dimensions of dendritic macromolecules were performed right from the start of the first synthesis of these highly branched species.<sup>1</sup> Issues of special interest with respect to the conformation of dendrimers include density profiles in the dendrimers, the localization of end-groups, and the limits of perfect dendrimer growth. The analytical prediction of de Gennes and Hervet,<sup>2</sup> using a self-consistent-field model, showed that dendrimers have all end groups at the periphery and the lowest density is in the core. Numerical calculations of Lesanec and Muthukumar predicted,<sup>3</sup> however, the presence of end groups throughout the dendrimer and the highest density at the core. The latter model is consistent with other theoretical studies, some of them suggesting a constant density in the dendrimer.<sup>4</sup>

Empirical studies on the dendritic box (DAB-dendr-(NH-L-Phe-*t*-BOC)<sub>64</sub>)<sup>5</sup> and related structures,<sup>6</sup> including NMR relaxation data,<sup>5</sup> exchange interactions between radical centers,<sup>7</sup> and (chir)-optical data,<sup>8</sup> showed that the model of de Gennes and Hervet is operative.<sup>9</sup> Also SANS studies on PAMAM dendrimers subscribe the presence of endgroups on the dendrimer surface.<sup>10</sup> However, experiments on other dendrimers, including solution NMR,<sup>11</sup> REDOR-NMR,<sup>12</sup> SEC,<sup>13</sup> SANS,<sup>14</sup> and viscosimetry studies presented firm evidence for the backfolding of dendritic branches in accordance with the second theoretical model. None of the

## Scheme 1

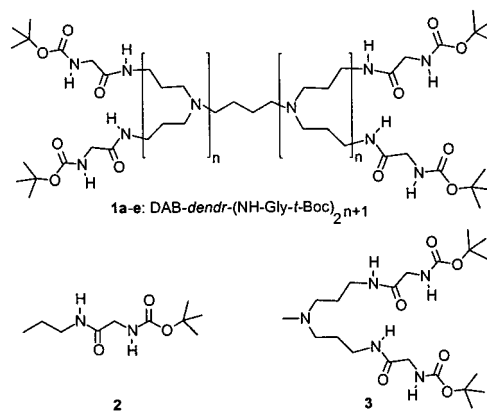


**Table 1.** Hydrogen-Bonding Data of **1a**<sup>a</sup>

| H-bonding type | atoms <sup>b</sup> | distance <sup>c</sup> | angle <sup>d</sup> |
|----------------|--------------------|-----------------------|--------------------|
| intramolecular | N102–O104          | 2.830(4)              | 144.7(2)           |
|                | N102–N103          | 2.782(5)              | 108.2(2)           |
|                | N104–O105          | 2.924(4)              | 161.6(2)           |
| intermolecular | N103–O101a         | 2.993(4)              | 157.2(2)           |
|                | N105–O101a         | 2.893(4)              | 159.9(2)           |

<sup>a</sup> Suffix a denotes symmetry operation,  $-x, 1/2 - y, -1/2 + z$ , estimated standard deviations in parentheses. <sup>b</sup> For atom numbering see Figure 1. <sup>c</sup> Distance donor–acceptor (Å). <sup>d</sup> Angle N–H...A (deg).

theoretical studies presented so far discriminates between dendrimers with and without specific secondary interactions within the structure. These results indicate that, as a result of secondary interactions between the end groups, the dendritic termini are forced in close proximity.

The different generations of *N-t*-BOC-protected glycine functionalized dendrimers **1a–e** (DAB-dendr-(NH-Gly-*t*-BOC)<sub>2n+1</sub>,  $n = 1–5$ , respectively) were prepared in analogy to the synthesis of the dendritic box,<sup>5</sup> by the reaction of the *N*-hydroxy succinimidyl ester of *N-t*-BOC glycine with the poly(propylene imine) dendrimers<sup>15</sup> (Scheme 1). Reference compounds **2** and **3** were synthesized from *n*-propylamine and 3,3'-diamino-*N*-methyl-di-propylamine, respectively. The presence of intramolecular hydrogen bonding of all compounds was studied with NMR and IR spectroscopy, while single crystals of **1a** were obtained from dichloromethane and analyzed by X-ray.<sup>16</sup>

First generation dendrimer **1a** adopts a globular structure in the solid state (Figure 1), with four C<sub>2</sub> symmetric molecules **1a** and eight molecules dichloromethane in the unit cell. All H-bond donors of the end group are involved in the H-bonding with the acceptor sites within the amido-carbamate end group of the same or a neighboring molecule. As a result, the end groups are assembled on one side of the structure and the core atoms are positioned at the other side. Two linear and two bifurcated intramolecular H-bonds are accompanied by four bifurcated intermolecular H-bonds per molecule (Table 1). The intermolecular hydrogen bonds link the molecules into an infinite two-dimensional network perpendicular to  $\bar{a}$ . All of the secondary

(15) de Brabander-van den Berg, E. M. M.; Meijer, E. W. *Angew. Chem., Int. Ed. Engl.* **1993**, *32*, 1308–1311.

(16) Crystal data for **1a**: C<sub>44</sub>H<sub>84</sub>N<sub>10</sub>O<sub>12</sub>·2CH<sub>2</sub>Cl<sub>2</sub>; colorless crystals with orthorhombic spacegroup *Ab̄a2* (no. 41) with  $a = 22.942(4)$  Å,  $b = 24.674(11)$  Å,  $c = 10.775(4)$  Å,  $V = 6099(4)$  Å<sup>3</sup>,  $Z = 4$ , 13 406 reflections measured, (150 K, Mo K $\alpha$  radiation,  $0.89^\circ < \theta < 27.5^\circ$ ) of which 3413 are independent. The structure was solved by automated direct methods (SHELXS96). Refinement on  $F^2$  (SHELXL-97), 331 parameters, with H-atoms at calculated positions.  $wR2 = 0.1384$ ,  $R1 = 0.0546$  for 2856  $I > 2\sigma(I)$ ,  $S = 1.046$ ,  $w = 1/[\sigma^2(F^2) + (0.0658P)^2 + 4.35P]$ , with  $P = (\text{Max}(F_o^2, 0) + 2F_c^2)/3$ . No residual density was found outside  $-0.50$  and  $0.47$  e Å<sup>-3</sup>.

<sup>†</sup> Eindhoven University of Technology.

<sup>‡</sup> Utrecht University.

(1) For an extensive review on dendrimers, see: (a) Newkome, G. R.; Moorefield, C. N.; Vögtle, F. *Dendritic Molecules*; VCH: Weinheim, 1996. (b) Tomalia, D. A.; Naylor, A.; Goddard, W. A. *Angew. Chem., Int. Ed. Engl.* **1990**, *29*, 138–175.

(2) de Gennes, P. G.; Hervet, H. *Phys. Lett.* **1983**, *44*, L-351–L-361.

(3) Lesanec, R. L.; Muthukumar, M. *Macromolecules* **1990**, *23*, 2280–2288.

(4) (a) Mansfield, M. L.; Klushin, L. I. *Macromolecules* **1993**, *26*, 4262–4268. (b) Murat, M.; Grest, G. S. *Macromolecules* **1996**, *29*, 1278–1285. (c) Boris, D.; Rubinstein, M. *Macromolecules* **1996**, *29*, 7251–7260.

(5) Jansen, J. F. G. A.; de Brabander-van den Berg, E. M. M.; Meijer, E. W. *Science* **1994**, *265*, 1226–1229.

(6) See also the spherical supramolecular dendrimers with a microsegregated model: Hudson, S. D.; Jung, H.-T.; Percec, V.; Cho, W.-D.; Johansson G.; Ungar, G.; Balagurusamy, V. S. K. *Science* **1997**, *278*, 449–452.

(7) Bosman, A. W.; Janssen, R. A. J.; Meijer, E. W. *Macromolecules* **1997**, *30*, 3606–3611.

(8) Jansen, J. F. G. A.; Peerlings, H. W. I.; de Brabander-van den Berg, E. M. M.; Meijer, E. W. *Angew. Chem., Int. Ed. Engl.* **1995**, *34*, 1206–1209.

(9) For recent calculations and simulations on the dendritic box and the encapsulation of guests therein, see: (a) Miklis, P.; Çagin, T.; Goddard, W. A., III. *J. Am. Chem. Soc.* **1997**, *119*, 7458–7462. (b) Cavallo, L.; Fraternali, F. *Chem. Eur. J.* **1998**, *4*, 927–934.

(10) (a) Prosa, T. J.; Bauer, B. J.; Amis, E. J.; Tomalia, D. A.; Scherrenberg, R. J. *Polym. Sci. B* **1997**, *35*, 2913–2924. (b) Amis, E. J.; Topp, A.; Bauer, B. J.; Tomalia, D. A. *Polym. Mater. Sci. Eng.* **1997**, *77*, 183–184.

(11) (a) Meltzer, A. D.; Tirrel, D. A.; Jones, A. A.; Ingfield, P. T.; Hedstrand, D. M.; Tomalia, D. A. *Macromolecules* **1992**, *25*, 4541–4548.

(12) Wooley, K. L.; Klug, C. A.; Tasaki, K.; Schaefer, J. *J. Am. Chem. Soc.* **1997**, *119*, 53–58.

(13) Mourey, T. H.; Turner, S. R.; Rubinstein, M.; Fréchet, J. M. J.; Hawker, C. J.; Wooley, K. L. *Macromolecules* **1992**, *25*, 2401–2406.

(14) Scherrenberg, R.; Coussens, B.; van Vliet, P.; Edouard, G.; Brackman, J.; de Brabander, E.; Mortensen, K. *Macromolecules* **1998**, *31*, 456–461.

**Table 2.** Solution Hydrogen-Bonding Data of **1–3**<sup>a</sup>

|   | <b>2</b> | <b>3</b> | DAB-dendr-(NH-Gly- <i>t</i> -BOC) <sub>2</sub> <sup>n+1</sup> |           |           |           |           |
|---|----------|----------|---|-----------|-----------|-----------|-----------|
|   |          |          | <b>1a</b>   | <b>1b</b> | <b>1c</b> | <b>1d</b> | <b>1e</b> |
| amount of H-bonding <sup>b</sup>                  | 0        | 0.61     | 0.67  | 0.70      | 0.77      | 0.79      | 0.80      |
| $\delta$ <i>sec</i> -amide (ppm)                  | 6.06     | 6.98     | 7.03  | 7.24      | 7.33      | 7.46      | 7.54      |
| $\delta$ carbamate (ppm)                          | 5.08     | 5.55     | 5.62  | 5.82      | 5.92      | 6.11      | 6.13      |
| $\Delta\delta/\Delta T$ <i>sec</i> -amide (ppb/K) | -3.4     | -5.1     | -7.8  | -8.3      | -8.0      | -7.4      | -6.4      |
| $\Delta\delta/\Delta T$ carbamate (ppb/K)         | -2.1     | -5.4     | -6.1  | -7.7      | -7.9      | -6.6      | -6.8      |

<sup>a</sup> FT-IR measurements performed in dichloromethane; NMR measurements in deuterated dichloromethane; all measurements performed in 0.5–3.2 mM concentration regime. <sup>b</sup> Values obtained from FT-IR spectra after subtraction of solvent spectrum and deconvolution of peaks;  $\epsilon = 1.32 \times 10^3 \text{ mm}^{-1} \text{ M}^{-1}$  for 3435  $\text{cm}^{-1}$  absorption in absence of H-bonding (see text).

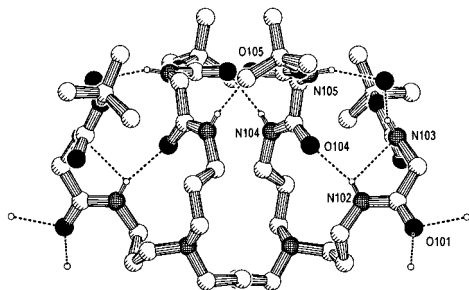


**Figure 1.** PLUTON representation of the crystal structure of DAB-dendr-(NH-Gly-*t*-BOC)<sub>4</sub>. Hydrogen bonds are shown by dotted lines, only protons involved in hydrogen bonding are shown for clarity. Acceptor atom O101 [ $-x, 1/2 - y, -1/2 + z$ ] as well as the donating hydrogen atoms of other neighboring molecules have been included to provide a complete scheme of all hydrogen bonding interactions.

interactions are located between carbonyls and N–H functions of different branches, while no interactions are found involving tertiary amines or nearest neighbor groups.<sup>17</sup> This finding is in sharp contrast to the X-ray structures of the Fréchet-type wedges, in which no end group interactions are present and there, the end groups are positioned away from each other as far as possible.<sup>18</sup>

The X-ray structure of **1a** supports the dense shell motif in the dendritic box in which all end groups interact intramolecularly. To confirm this proposal, we have studied all molecules in solution. IR spectroscopy of **1–3** in dichloromethane (1 mM) shows both one absorption at 3435  $\text{cm}^{-1}$  for non H-bonded amide and carbamate N–H stretching vibrations and one broad absorption at approximately 3320  $\text{cm}^{-1}$  for the H-bonded amide and carbamate N–H stretching vibrations.<sup>17,19</sup> Integration of both absorptions yields the relative amount of H-bonded species (Table 2).<sup>20</sup> These H-bond interactions are only intramolecular, since the ratio of both peaks is not changed upon dilution of the starting

solution.<sup>21</sup> There is an increase in the amount of intramolecular H-bonding in going to dendrimers of higher generation, attributed to a increase in the local concentration of end groups, that are forced in closer proximity. From the data, we estimate a  $K_{\text{eq}}$  of  $1.6 \pm 0.1$  for model compound **3**, which is comparable to bipeptide systems reported before.<sup>20</sup>

<sup>1</sup>H NMR measurements in deuterated dichloromethane have been performed to discriminate between the N–H resonances of the amide and the carbamate. Both N–H resonances shift to lower field by going to higher generations (Table 2). Comparable shifts have been found for poly(propylene imine) dendrimers functionalized with amide groups only.<sup>5,22</sup> Following the methods developed by Gellman et al.<sup>19</sup> to establish the equilibrium constants of the intramolecular bonding in **3**, we estimate  $K_{\text{eq}} = 0.8$  for the amide and  $K_{\text{eq}} = 0.3$  for the carbamate, which are in good agreement with the IR measurements. Measurements of the reduced temperature coefficients ( $\Delta\delta/\Delta T$ ) confirm that the observed differences in H-bonding originate from the closer proximity of the end groups.

In conclusion, the X-ray structure of **1a** shows multiple interactions between the different end groups of the dendrimer, modeling the shell of a higher generation dendrimer. Spectroscopic results from solutions of dendrimers of all generations confirm this close proximity of end groups. Therefore, we conclude that the answers to questions concerning density profiles in dendrimers, localization of end groups, and related issues are highly dependent on the structure of the dendrimer and suggest the need to revisit the theoretical models by taking into account the possibilities of secondary interactions.

**Acknowledgment.** This work was supported by The Netherlands Foundation for Chemical Research (SON) with financial aid from The Netherlands Organization for Scientific Research (NWO). DSM Research is acknowledged for an unrestricted research grant.

**Supporting Information Available:** Details of the synthesis and characterization of **1a–e**, **2** and **3**, infrared spectra, and atomic displacement ellipsoid plot for **1a** (7 pages, print/PDF). An X-ray crystallographic file of **1a**, in CIF format, is available via the Web only. See any current masthead page for ordering information and Web access instructions.

JA981626G

(21) Highly concentrated solution, however, showed a small increase of H-bonding, but only for the model compounds and the lower generations **1a–c**.

(22) (a) Put, E. J. H.; Clays, K.; Persoons, A.; Biemans, H. A. M.; Luijckx, C. P. M.; Meijer, E. W. *Chem. Phys. Lett.* **1996**, *269*, 136–141. (b) Stevelmans, S.; van Hest, J. C. M.; Jansen, J. F. G. A.; van Boxtel, D. A. F. J.; de Brabander-van den Berg, E. M. M.; Meijer, E. W. *J. Am. Chem. Soc.* **1996**, *118*, 7398–7399.

(17) Néel, J. *Pure Appl. Chem.* **1972**, *31*, 201–225.

(18) (a) Ferguson, G.; Gallagher, J. F.; McKervey, M. A.; Madigan, E. *J. Chem. Soc., Perkin Trans. 1* **1996**, 599–602. (b) Karakaya, B.; Claussen, W.; Gessler, K.; Saenger, W.; Schlüter, A.-D. *J. Am. Chem. Soc.* **1997**, *119*, 3296–3301.

(19) Gellman, S. H.; Dado, G. P.; Liang, G.-B.; Adams, B. R. *J. Am. Chem. Soc.* **1991**, *113*, 1164–1173. We used  $\delta$  5.94 and 8.29 ppm for non H-bonded and fully H-bonded amide in **2**, respectively, and 5.04 and 7.14 ppm for the non and fully H-bonded carbamate in **2**, respectively.

(20)  $K_{\text{eq}} = [\text{H-bonded}]/[\text{non H-bonded}]$ , for determination of amount of hydrogen bonding, see: Gardner, R. R.; Gellman, S. H. *J. Am. Chem. Soc.* **1995**, *117*, 10411–10412. Amide and carbamate functions have comparable extinction coefficients, see: Katritzky, A. R.; Jones, R. A. *J. Chem. Soc.* **1959**, 2067–2071; **1960**, 676–679.